CARBON 53 (2013) 374–379

Available at www.sciencedirect.com

SciVerse ScienceDirect

journal homepage: www.elsevier.com/locate/carbon

Laser direct synthesis of graphene on quartz

Dapeng Wei [a], *James I. Mitchell* [a], *Chookiat Tansarawiput* [b], *Woongsik Nam* [a], *Minghao Qi* [b], *Peide D. Ye* [b], *Xianfan Xu* [a,*]

[a] *School of Mechanical Engineering, Birck Nanotechnology Center, Purdue University, West Lafayette, IN 47907, USA*
[b] *School of Electrical and Computer Engineering, Birck Nanotechnology Center, Purdue University, West Lafayette, IN 47907, USA*

ARTICLE INFO

Article history:
Received 5 July 2012
Accepted 12 November 2012
Available online 20 November 2012

ABSTRACT

We demonstrate a laser-based technique to directly synthesize few layer graphene on quartz substrates without using any metal catalyst. In our approach, a photoresist S-1805 (from Shipley Comp.) film coated on quartz wafers was heated, and then decomposed, by irradiation of a continuous-wave laser. The carbon atoms from the photoresist were dissolved in the molten quartz, and then extracted to form graphene when the temperature of the quartz was decreased. Raman spectroscopy shows the as-produced graphene is two to three layers thick. This laser-based method will provide a new approach and platform for applications of graphene-based devices.

1. Introduction

Graphene, a crystal of carbon atoms arranged in a honeycomb lattice, is emerging as an ideal material for future electronic devices [1–3]. Due to its outstanding electronic transport properties including high carrier mobility and perfect charge carrier confinement [4,5], graphene holds promises for a wide range of applications including field-effect transistors, supercapacitors, and sensors [6–8]. So far, the main routes for preparing graphene are mechanical exfoliation and chemical vapor deposition (CVD), and large-scale graphene is grown on Cu or Ni surfaces [9,10]. For device fabrication, the graphene grown on Cu or Ni needs to be transferred onto another insulating substrate [11], which carries the risk of contamination.

Here we describe a laser-based method for synthesizing graphene directly on an insulating substrate, quartz. Therefore, the as-grown graphene is ready to be used for device fabrication. Laser-based method is in general an attractive alternative for materials synthesis, with the intrinsic benefits of localized, fast, and single-step process [12–15]. Different from the conventional thermal CVD approach, a focused laser beam can produce the required temperature and chemical reaction in a confined area, while the rest of the material (substrate) remains at the room temperature. Recently, it has been reported that laser technique can be used for growing graphene on nickel [14], and for epitaxially growing graphene on SiC [13]. In a previous work, we successfully grew few layer graphene on a silicon substrate using laser-based technique without any metal catalysts [16]. These laser-based methods produce graphene on a conductive substrate, and a transfer process onto an insulating substrate is therefore needed for fabricating a graphene device.

In this communication, we report the development of a laser-based technique for synthesizing graphene without any metal catalysts on an insulating substrate, quartz. This laser-induced growth route is schematically illustrated in Fig. 1. A solid film containing carbon such as a photoresist was coated on quartz by spin-coating. The film was heated, and then decomposed, by irradiation of a focused continuous wave laser beam. The carbon atoms were dissolved in the molten quartz, and then extracted to form graphene when the temperature of quartz was decreased. The sample was mounted on a high precision piezoelectric stage and a DC motorized stage, therefore, the location of the graphene growth can be precisely controlled.

* *Corresponding author:* Fax: +1 765 494 0539.
E-mail address: xxu@purdue.edu (X. Xu).
0008-6223/$ - see front matter
http://dx.doi.org/10.1016/j.carbon.2012.11.026

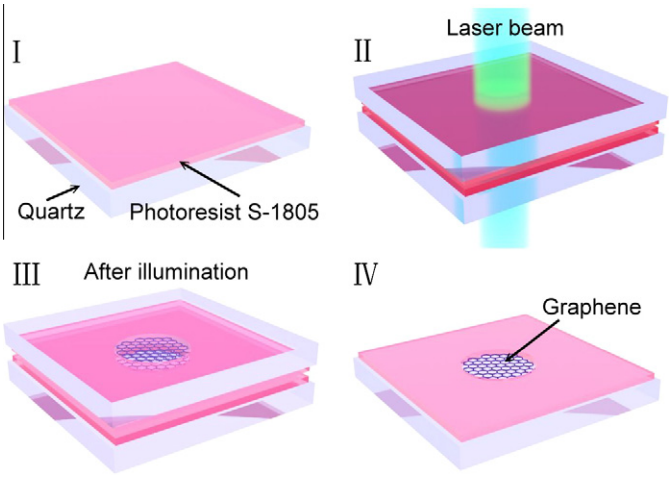

Fig. 1 – Schematic diagram of laser-induced growth of graphene on quartz wafer.

2. Experimental

2.1. Synthesis of graphene

Two 1×2 cm quartz wafers were used as substrate to grow graphene. The quartz wafers were first cleaned by ultrasonication in methanol, acetone, and DI water, and were dried by high purity N_2 gas. Photoresist S-1805 (from Shipley Comp.) was diluted with a volume ratio of 1:6 in Thinner-P (from MicroChem Corp.), and was then spin-coated on the quartz wafer at 10,000 rpm. The thickness of the coated film is about 30 nm. The photoresist-coated quartz wafers were then baked for 5 min at 120 °C. One coated quartz wafer was covered by another piece of quartz wafer, and then mounted on a sample stage in a vacuum chamber. Before growing graphene, the chamber was pumped and purged by high-purity N_2 gas, and maintained at a pressure below 0.1 Torr. A continuous wave (CW) Nd:YAG laser with a wavelength of 532 nm was focused on the S-1805 film through the transparent quartz substrate using a lens of 150 mm focal length. The carbon atoms were decomposed from the laser heated photoresist, then dissolved in the molten quartz, and extracted to form graphene when the temperature of quartz was decreased. With our optical setup, the graphene was produced with a laser power of 2.8 W, irradiated for 3–5 min.

2.2. Characterization methods

Optical images were taken with a microscope in a reflection mode. Atomic force microscopy (AFM) images were taken using an AFM (Veeco Dimension 3100) operated with the tapping mode under ambient conditions. Raman spectroscopy and mapping were performed using a micro-Raman system (XploRA) equipped with a motorized sample stage with laser excitation at 532 nm. A 100× objective lens was used to produce a laser spot size of about 0.6 μm in diameter, and the accumulation time was 20 s. Each spectrum was an average of three acquisitions, 3 s of accumulation time per acquisition. For electrical measurements, electrodes (Ti/Au, 20 nm/80 nm) were patterned using e-beam lithography. Sheet resistance of graphene was obtained by 2-point current–voltage (*I*–*V*) measurement and 4-point Van der Pauw method at the room temperature.

3. Results and discussion

Fig. 2a shows an optical micrograph of a 4×4 laser processed areas where graphene is grown, with a spacing of 250 μm. The graphene are shown as visible, round dots with bright rings. The diameter of the graphene dots is about 50 μm. The higher magnification optical micrograph in Fig. 2b shows uniformity and smoothness of laser-irradiated areas with a clear boundary inside bright rings, whose brightness gradually decreases along radial direction. The bright ring is in fact a ridge which is higher than the other area by about 300 nm. This type of ridge structure is typical during laser melting, caused by surface tension in a molten material irradiated by a laser beam [17,18]. An AFM image of the central laser-irradiated area is shown in Fig. 2c, within which the surface height varies within 1–2 graphene layer height (0.6–1.2 nm).

The nature and quality of graphene formed by laser irradiation were evaluated using Raman spectroscopy. The hallmarks of graphene are the three Raman peaks in the D (~1350 cm^{-1}), G (~1580 cm^{-1}), and 2D (~2700 cm^{-1}) bands [19,20]. The D band is the so-called defect band of graphene, and the intensity ratio of D to G bands, I_D/I_G, is a parameter to identify disorder in graphene [21,22]. The 2D band is the most prominent feature in the Raman spectra of graphene, and its position, shape, I_{2D}/I_G intensity ratio, and full width at half-maximum (FWHM) are well-established characteristics of graphene layers [10,23,24]. The Raman mapping with the I_D/I_G and I_{2D}/I_G ratios are shown in Fig. 3, panels a and b, respectively. The central circular area shows low I_D/I_G (0.1–0.2) and high I_{2D}/I_G (0.7–1.0) ratios, and its size is similar to the size of laser-processed area. Hence, the growth of graphene only happens in the laser-processed area. The Raman spectra shown in Fig. 3c correspond to the points marked by "A", "B" and "C" in Fig. 3a. There is no signal of the 2D band outside the laser processed area; instead, the wide and strong D and G bands reveal sp^2-rich amorphous carbon on the surface [25,26]. For typical Raman spectra in the laser processed area, the position of the 2D band at

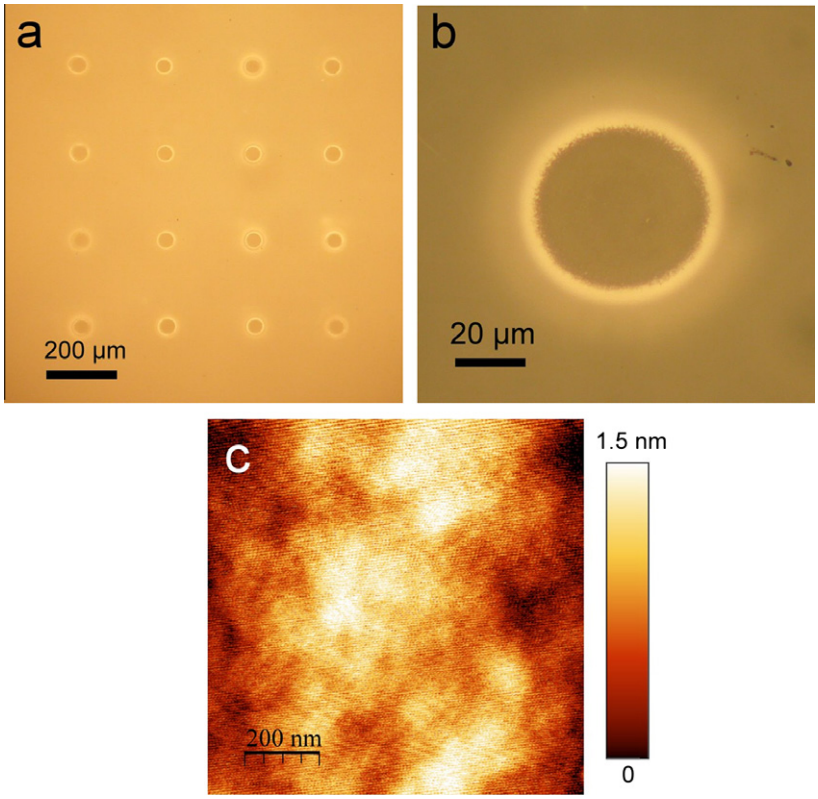

Fig. 2 – (a) Optical micrograph of 4 × 4 graphene dot arrays with the spacing of 250 μm, (b) a magnified optical micrograph of a graphene dot, (c) an AFM image of the central area of a graphene dot.

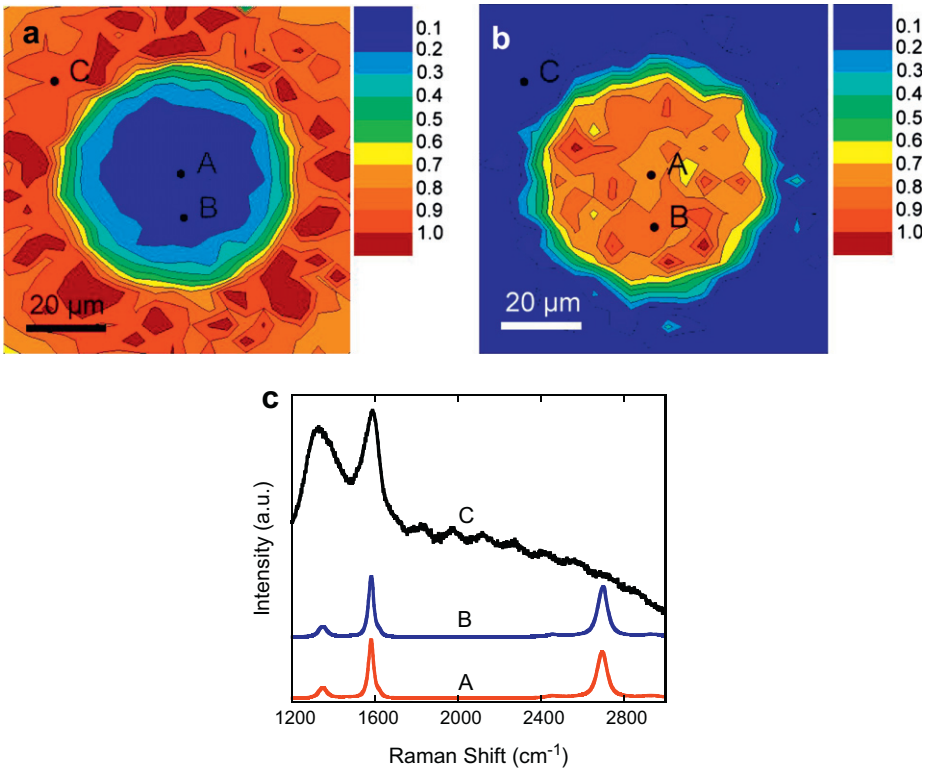

Fig. 3 – Typical Raman mapping of (a) I_D/I_G and (b) I_{2D}/I_G in the laser-processed area, (c) the Raman spectra from the marked points in (a) and (b).

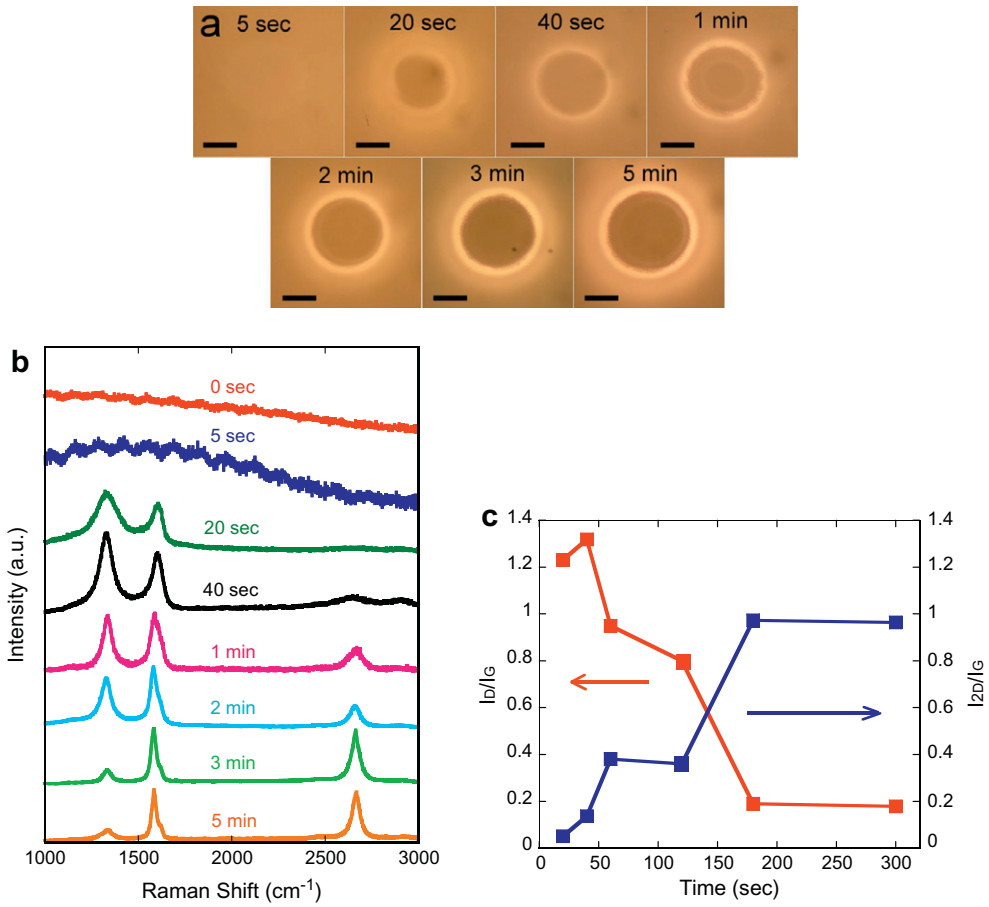

Fig. 4 – (a) Optical micrographs of laser-irradiated areas. The laser power is 2.8 W, and the illumination time is 0 s, 5 s, 20 s, 40 s, 1 min, 2 min, 3 min, and 5 min. All of the scale bars are 20 μm. (b) The corresponding Raman spectra recorded from the center of the laser-irradiated areas in (a). (c) The intensity ratios I_D/I_G and I_{2D}/I_G of graphene dots as a function of growth time.

2696 cm^{-1} and the FWHM (2D) of 58 cm^{-1} are different from the 2D band position of monolayer graphene at 2680 cm^{-1} and FWHM (2D) of 30 cm^{-1} [10,12,23]. Up-shifted and wider 2D band indicates the laser produced graphene have bi- or tri-layer structures.

The I_{2D}/I_G ratio from 0.7 to 1.0 also indicates that the graphene has bi- or tri-layer structure [10,23,27]. On the other hand, the I_D/I_G ratio is an indication of the graphene crystallite sizes, L_a (nm), which can be estimated as $L_a = (2.4 \times 10^{-10})\ \lambda_1^4\ (I_D/I_G)^{-1}$, where λ_1 is the Raman laser line wavelength in nanometers x[28,29]. From the experimental data, the I_D/I_G ratio from 0.1 to 0.2 corresponds to the graphene domain size between 96 nm and 192 nm.

In the commonly used CVD approach for growing graphene on metals, the growth parameters such as temperature and pressure are basic factors that determine the formation and quality of graphene film [30,31]. In our case, the process is controlled by absorption of the laser beam and the resulting heating. The quartz substrate is transparent to the laser wavelength (532 nm). The photoresist S-1805 is a light-sensitive organic mixture of photoactive compound, resin, solvent and some additives, and can absorb a part of power of 532 nm laser, although its main absorption happens at the ultraviolet band. The photoresist also provides carbon for the growth of graphene [16,32]. When the laser power is high enough, the photoresist is decomposed, and the heat transferred to quartz melts the quartz surface. As mentioned previously, deformation of the laser-processed area suggests that the surface experienced melting during the formation of graphene. Therefore, the growth of graphene on quartz is not the same as the surface-catalyzed process [33] or carbon dissolution and precipitation in solid metal [34] when graphene is grown on metal.

From our experiments, it was found that the laser power and the thickness of the photoresist film directly determined the temperature and the quality of graphene. Using laser power lower than 2.8 W did not produce sufficient temperature and there was no graphene growth. Similarly, a thinner photoresist film (~20 nm) did not absorb enough laser power for producing graphene. On the other hand, using higher laser power (with less heating time) or thicker photoresist film (40 nm or thicker) will produce much higher temperature and the resulting surface appears to be rough. Therefore, the laser power and the thickness of the photoresist film were empirically optimized.

Fig. 4a displays optical microscopy images of laser-irradiated areas with different laser irradiation times, which show the formation process of graphene on quartz. Within the first 5 s, the surface had no visible change. After 20 s, the bright rings started to appear, and gradually became more visible.

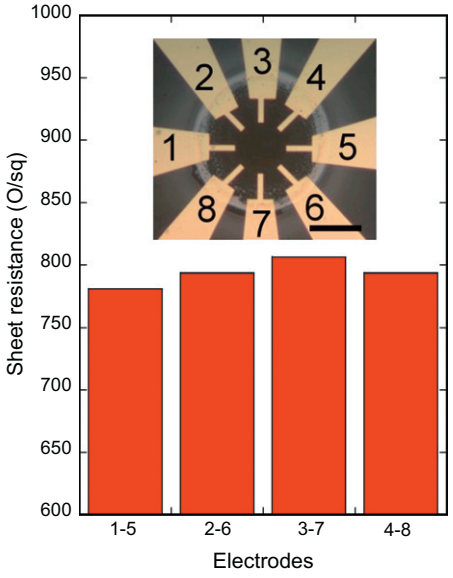

Fig. 5 – Sheet resistances between different electrodes. The inset: the optical micrograph of graphene with multiple electrodes (numbered 1–8). The scale bar is 20 μm.

Meanwhile, the diameter of the rings increased continuously, and reached ~50 μm at 5 min. Fig. 4b shows the corresponding Raman spectra recorded from the centers of laser irradiated areas. At 5 s, no D, G or 2D Raman bands were detected, and some disordered Raman signals might result from the fragments from decomposition of S-1805. At 20 s, broad D and G bands appeared, but the 2D band was invisible. After 40 s, the 2D band started to appear, and its height increased continuously until 3 min. Meanwhile, the D band became weaker and narrower. Between 3 and 5 min, the Raman spectra changed little. Fig. 4c shows the I_D/I_G and I_{2D}/I_G ratios as a function of laser processed time. Clearly, the graphene domain size was increasing gradually with laser illumination time, indicating the graphene crystallization process. After illuminated for 3 min, 2–3 layer graphene was formed. Irradiation for more than 5 min resulted in more than 3 layers of graphene (not shown).

The Raman spectra in Fig. 4 suggest the mechanism of graphene growth. First, the focused laser beam raised the temperature in the S-1805 film, drove the decomposition of S-1805 to form amorphous carbon and carbon vapor, and melted the quartz surface. Some carbon atoms diffused into the melted quartz. During cooling, the dissolved carbon atoms were separated and nucleated. These precipitated carbon formed graphene segments, because sp^2-bonded graphene is energetically more favorable than sp^3-rich amorphous carbon [35,36], and then grew to form larger size crystals. Finally, these graphene crystals were coalesced to form continuous graphene film.

In order to evaluate electrical conductivity of the graphene film grown on quartz, multiple electrodes were fabricated using e-beam lithography. The spacing between the opposite electrodes was 20 μm, as shown in the inset of Fig. 5. The current–voltage (*I–V*) measurements between opposite electrodes were performed, and the sheet resistances were found to be in the range of 780–805 Ω/sq. These values are comparable to those obtained from wet-transferred graphene (650–900 Ω/sq) and chemically reduced graphene oxide (700–1300 Ω/sq) [37,38], lower than those of Cu-catalyzed graphene (50–75 Ω/sq) [39], and better than Ni-catalyzed graphene (6–11 kΩ/sq) and catalyst-free nano-graphene (7–11 kΩ/sq) [40,41]. Therefore, the laser-grown graphene will have potential applications similar to those prepared by other methods.

4. Summary

A single-step laser-based method was developed to directly synthesize few-layer graphene arrays on quartz wafer. This process does not require use of any metal catalysts. The melted quartz absorbs and dissolves carbon atoms which are decomposed from the photoresist from laser heating. The dissolved carbon atoms were extracted from the melted quartz during the cooling and resolidification process to form graphene. The sheet resistance of the as-grown graphene is in the range of 780–805 Ω/sq. This simple, rapid, single-step, and controllable method for synthesizing graphene will have a significant impact on the graphene-device fabrication and applications.

Acknowledgements

We acknowledge the support of the Defense Advanced Research Projects Agency (Grant No. N66001-08-1-2037) and the National Science Foundation (Grant No. CMMI-1120577).

REFERENCES

[1] Allen MJ, Tung VC, Kaner RB. Honeycomb carbon: a review of graphene. Chem Rev 2010;110:132–45.
[2] Novoselov KS, Geim AK, Morozov SV, Jiang D, Katsnelson M, Dubonos SV, et al. Two-dimensional gas of massless dirac fermions in graphene. Nature 2005;438:197–200.
[3] de Heer WA. Epitaxial graphene: a new electronic material for the 21st century. MRS Bull 2011;36:632–9.
[4] Morozov SV, Novoselov KS, Katsnelson MI, Schedin F, Elias DC, Jaszczak JA. Giant intrinsic carrier mobilities in graphene and its bilayer. Phys Rev Lett 2008;100. 016602-1–4.
[5] Berger C, Song ZM, Li XB, Wu XS, Brown N, Naud C, et al. Electronic confinement and coherence in patterned epitaxial graphene. Science 2006;312:1191–6.
[6] Schwierz F. Graphene transistors. Nat Nanotechnol 2010;5:487–96.
[7] Liu CG, Yu ZN, Neff D, Zhamu A, Jang BZ. Graphene-based supercapacitor with an ultrahigh energy density. Nano Lett 2010;10:4863–8.
[8] Liu YX, Dong XC, Chen P. Biological and chemical sensors based on graphene materials. Chem Soc Rev 2012;41:2283–307.
[9] Novoselov KS, Geim AK, Morozov SV, Jiang D, Zhang Y, Dubonos SV, et al. Electric field effect in atomically thin carbon films. Science 2004;306:666–9.
[10] Li XS, Cai WW, An JH, Kim S, Nah J, Yang DX, et al. Large-area synthesis of high-quality and uniform graphene films on copper foils. Science 2009;324:1312–4.

[11] Kim KS, Zhao Y, Jang H, Lee SY, Kim JM, Kim KS, et al. Large-scale pattern growth of graphene films for stretchable transparent electrodes. Nature 2009;457:706–10.
[12] Park JB, Jeong SH, Jeong MS, Lim SC, Lee IH, Lee YH. The rapid growth of vertically aligned carbon nanotubes using laser heating. Nanotechnology 2009;20. 185604-1–7.
[13] Lee S, Toney MF, Ko W, Randel JC, Jung HJ, Munskata K, et al. Laser-synthesized epitaxial graphene. ACS Nano 2010;4:7524–30.
[14] Park JB, Xiong W, Gao Y, Qian M, Xie ZQ, Mitchell M, et al. Fast growth of graphene patterns by laser direct writing. Appl Phys Lett 2011;98. 123109-1–3.
[15] Hwang DJ, Ryu SG, Grigoropoulos CP. Multi-parametric growth of silicon nanowires in a single platform by laser-induced localized heat sources. Nanotechnology 2011;22. 385303-1–11.
[16] Wei DP, Xu X. Laser direct growth of graphene on silicon substrate. Appl Phys Lett 2012;100. 023110-1–3.
[17] Willis DA, Xu X, Poon CC, Tam AC. Laser-assisted surface modification of thin chromium films. Opt Eng 1997;37:1033–41.
[18] Willis DA, Xu X. Transport phenomena and droplet formation during pulsed laser interaction with thin films. J Heat Trans 2000;122:763–70.
[19] Malard LM, Pimenta MA, Dresselhaus G, Dresselhaus MS. Raman spectroscopy in graphene. Phys Rep 2009;473:51–87.
[20] Tang B, Guoxin H, Gao HY. Raman spectroscopic characterization of graphene. Appl Spectrosc Rev 2010;45:367–407.
[21] Cancado LG, Jorio A, Ferreira EHM, Stavale F, Achete CA, Capaz RB, et al. Quantifying defects in graphene via Raman spectroscopy at different excitation energies. Nano Lett 2011;11:3190–6.
[22] Pimenta MA, Dresselhaus G, Dresselhaus MS, Cancado LG, Jorio A, Saito R. Studying disorder in graphite-based systems by Raman spectroscopy. Phys Chem Chem Phys 2007;9:1276–91.
[23] Reina A, Jia XT, Ho J, Nezich D, Son HB, Bulovic V. Large area, few-layer graphene films on arbitrary substrates by chemical vapor deposition. Nano Lett 2009;9:30–5.
[24] Ferrari AC, Meyer JC, Scardaci V, Casiraghi C, Lazzeri M, Mauri F, et al. Raman spectrum of graphene and graphene layers. Phys Rev Lett 2006;97. 187401-1–4.
[25] Zheng M, Takei K, Hsia B, Fang H, Zhang XB, Ferralis N, et al. Metal-catalyzed crystallization of amorphous carbon to graphene. Appl Phys Lett 2010;96. 063110-1–3.
[26] Scheibe HJ, Drescher D, Alers P. Raman characterization of amorphous carbon films. Fresenius J Anal Chem 1995;353:695–7.
[27] Cao HL, Yu QK, Colby R, Pandey D, Park CS, Lian J, et al. Large scale graphitic thin films synthesized on Ni and transferred to insulators Structural and electronic properties. J Appl Phys 2010;107. 044310-1–7.
[28] Cancado LG, Takai K, Enoki T, Endo M, Kim YA, Mizusaki H, et al. General equation for the determination of the crystallite size La of nanographite by Raman spectroscopy. Appl Phys Lett 2006;88. 163106-1–3.
[29] Rümmeli MH, Bachmatiuk A, Scott A, Borrnert F, Warner JH, Hoffman V, et al. Direct low-temperature nanographene CVD synthesis over a dielectric insulator. ACS Nano 2010;4:4206–10.
[30] Li XS, Magnuson CW, Venugopal A, An JH, Suk JW, Han BY, et al. Graphene films with large domain size by a two-step chemical vapor deposition process. Nano Lett 2010;10:4328–34.
[31] Bhaviripudi S, Jia XT, Dresselhaus MS, Kong J. Role of kinetic factors in chemical vapor deposition synthesis of uniform large area graphene using copper catalyst. Nano Lett 2010;10:4128–33.
[32] Sun ZZ, Yan Z, Yao J, Beitler E, Zhu Y, Tour JM. Growth of graphene from solid carbon sources. Nature 2010;468: 549–52.
[33] Yu QK, Jauregui LA, Wu WW, Colby R, Tian JF, Su ZH, et al. Control and characterization of individual grains and grain boundaries in graphene grown by chemical vapour deposition. Nat Mater 2011;10:443–9.
[34] Yu QK, Lian J, Siriponglert S, Li H, Chen YP, Pei SS. Graphene segregated on Ni surfaces and transferred to insulators. Appl Phys Lett 2008;93. 113103-1–3.
[35] Reznik A, Richter V, Kalish R. Kinetics of the conversion of broken diamond (sp^3) bonds to graphitic (sp^2) bonds. Phys Rev B 1997;56:7930–4.
[36] Kahng YH, Chio J, Park BC, Kim DH, Choi JH, Lyou J, et al. The role of an amorphous carbon layer on a multi-wall carbon nanotube attached atomic force microscope tip in making good electrical contact to a gold electrode. Nanotechnology 2008;19. 195705-1–7.
[37] Li X, Zhu Y, Cai W, Borysiak M, Han B, Chen D, et al. Transfer of large-area graphene films for high-performance transparent conductive electrodes. Nano Lett 2009;9:4359–63.
[38] Zhao J, Pei S, Ren W, Gao L, Cheng HM. Efficient preparation of large-area graphene oxide sheets for transparent conductive films. ACS Nano 2010;4:5245–52.
[39] Bae S, Kim H, Lee Y, Xu X, Park JS, Zheng Y, et al. Roll-to-roll production of 30-inch graphene films for transparent electrodes. Nat Nanotechnol 2010;5:574–8.
[40] Park HJ, Meyer J, Roth S, Skákalová V. Growth and properties of few-layer graphene prepared by chemical vapor deposition. Carbon 2010;48:1088–94.
[41] Zhang L, Shi Z, Wang Y, Yang R, Shi D, Zhang G. Catalyst-free growth of nanographene films on various substrates. Nano Res 2011;4:315–21.